CONF-9411198--1

Design and fabrication of a diamond-turned hybrid diffractive/refractive singlet for visible applications at ORNL

B. E. Bernacki, A. C. Miller, and L. C. Maxey
Oak Ridge National Laboratory
Oak Ridge, Tennessee 37831

In support of work performed by Martin Marietta Energy Systems, Inc., for the U.S. Department of Energy under contract DE-AC05-84OR21400

Design and fabrication of a diamond-turned hybrid diffractive/refractive singlet for visible applications at ORNL

B. E. Bernacki, A. C. Miller, and L. C. Maxey
Oak Ridge National Laboratory
Oak Ridge, Tennessee 37831

Abstract

Hybrid diffractive/refractive optics can be fabricated using traditional lithographic methods involving masks or holographic techniques as well as direct-write approaches that include electron-beam lithography, single-point diamond turning, and laser beam lithography. Only the direct-write methods have proven to be practical in producing continuous-form diffractive surfaces, or kinoforms, and among these methods, only diamond turning can easily produce large kinoforms on curved base surfaces. In this paper, we describe design and fabrication issues for a hybrid singlet produced by single-point diamond turning that functions in the visible portion of the spectrum and takes advantage of all of the degrees of freedom available from diamond turning: aspheric front surface to control spherical aberration, curved rear surface for elimination of coma, and kinoform surface placed on either curved base surface for control of primary chromatic aberration.

1. Introduction

Design of hybrid diffractive/refractive optics is typically treated analytically in the literature, and while single-point diamond turning is acknowledged as a promising method of fabrication, construction details for these devices are often ignored or dismissed as an exercise for the reader, with the exception of a few authors[1,2]. In practice, lens design is usually done with commercially-available software to take advantage of sophisticated optimization methods rather than resorting to the few special cases treated analytically in the literature. With recourse to commercial lens design software, the fabrication of a hybrid singlet is significantly more challenging than its design. In undertaking a project at ORNL to design, fabricate, and test a hybrid singlet for use in the visible, it was necessary to review the open literature to assess the state of the art in hybrid optical design and fabrication, and this paper summarizes that search. We review the main points necessary to design and fabricate a hybrid singlet, including the first-order predesign of a hybrid singlet, present the results of the first order design calculations using a commercial lens design program[3], present an approach for converting the diffractive phase function into a form amenable to diamond turning, and also review important fabrication issues, such as tool selection and feed rate for optimum surface finish.

2. Hybrid Singlet Predesign

Practical optical design is usually done with commercial software based on optimization methods, since closed form solutions are often unattainable. However, it is still instructive (and provides a good starting point for the lens design software) to perform a first order predesign so that one can have confidence in the design found by the computer software.

The classical design of an achromat requires the combination of two lenses made of glasses with different dispersive qualities and opposite powers to achieve acceptable performance over a specified band of wavelengths. The key to hybrid optics lies in the complementary dispersive properties of refractive and diffractive optics: in diffractive optics, the focal length varies directly with wavelength, while a refractive optic's focal length varies inversely with wavelength. Using a single glass type, the focal lengths of the refractive and diffractive elements can be made to coincide only at the design

wavelength. For both the traditional and hybrid approach, the achromat has a common focus for the two extreme wavelengths that define the band edges, with the center wavelength slightly out of focus. This residual chromatic aberration is termed secondary spectrum[4]. Due to the nature of optical glasses, this residual chromatic aberration with shift the focus about 1/2400 of the design focal length, but secondary spectrum can be several orders of magnitude greater for a hybrid lens, as will be shown later.

The long, short, and middle design wavelengths are defined as λ_L, λ_S, and λ_M, respectively. The reciprocal dispersive power for the refractive portion of the hybrid lens, or Abbe number, is defined as:[5]

$$(1) \qquad \nu_R = \frac{n_M - 1}{n_L - n_S}$$

and the subscripts denote the short, middle and long wavelengths at which the index of refraction was measured. Similarly, an effective Abbe number for the diffractive surface can be expressed as[6]

$$(2) \qquad \nu_D = \frac{\lambda_M}{\lambda_L - \lambda_S}.$$

Traditionally the F (hydrogen), d (helium), and C (hydrogen) spectroscopic lines have been used for measuring the index of refraction of glasses at the short (0.48613 μm), middle (0.58756 μm), and long (0.65627 μm) wavelengths. Acrylic will be used for fabrication of this hybrid singlet, and the value for the index of refraction for acrylic is 1.491 at the middle wavelength. The refractive and diffractive Abbe numbers are 57.2 and -3.45, respectively. The smaller the Abbe number, the more dispersive the material, while the sign denotes the sense of the dispersion. The thin-lens design equations the lenses-in-contact achromat are found in numerous optics texts[7], and are listed below. The result is two equations in two unknowns.

$$(3) \qquad \begin{aligned} \Phi_{total} &= \Phi_D + \Phi_R \\ 0 &= \frac{\Phi_D}{\nu_D} + \frac{\Phi_R}{\nu_R} \end{aligned}$$

Solving for the necessary refractive and diffractive powers needed for each element the result is

$$(4) \qquad \begin{aligned} \Phi_R &= -\frac{\nu_R}{\nu_D - \nu_R}\Phi_{total} \\ \Phi_D &= \frac{\nu_D}{\nu_D - \nu_R}\Phi_{total}. \end{aligned}$$

Expressed in focal lengths rather than power these equations become

$$(5) \qquad \begin{aligned} f_R &= -\frac{\nu_D - \nu_R}{\nu_R} f_{total} \\ f_D &= \frac{\nu_D - \nu_R}{\nu_D} f_{total}. \end{aligned}$$

Note that the focal length of each surface is positive, and larger than the overall focal length of the lens. In particular, the diffractive portion will have a fairly long focal length, which reduces the number of annular zones that will eventually have to be machined. Our singlet will be an F/3.6 optic having a 25

mm diameter. This sets the design focal length at 90 mm for the thin lens solution. Using the expressions above, refractive and diffractive focal lengths of 95.4 mm and 1582.2 mm are found. By making use of the paraxial expression for focal length, the radius of curvature for the refractive portion of the hybrid lens is found to be:

$$R = (n_d - 1) f_R = (1.491 - 1) \cdot 95.4 \text{ mm} = 46.8 \text{ mm}. \tag{6}$$

In the next section, we introduce the diffractive phase function and the concept of equivalent parent refractive surface and show how the calculation for the Fresnel zone locations allows us to determine the radius of the parent refractive surface as a function of the design focal length of the kinoform.

2.1 Diffractive Phase Function

Most modern lens design software permits the use of diffractive or binary surfaces, and can calculate the required form of the phase function produced by the diffractive surface using the facilities of the programs' optimization function. This phase function is typically expressed as

$$\Phi = \frac{2\pi}{\lambda_0} \cdot \sum_i \alpha_i \cdot \rho^{2i} \tag{7}$$

for a rotationally symmetric diffractive surface. The designer typically has the choice of how many terms to specify. For an F/3.6 hybrid optic, the first term will suffice for achromatization since most of the optical power is concentrated in the refractive element. To see how the α_i terms map into more familiar optical parameters, it is instructive to review the origin of the phase function, since it will eventually help us to determine how the optic should actually be fabricated by diamond turning.

At infinite conjugates, the difference in phase produced by a Fresnel zone plate having design focal length f_D and formed on a plane base surface can be expressed as:

$$\Delta\phi(\rho) = \frac{2\pi}{\lambda_0}\left(f_D - \sqrt{f_D^2 + \rho^2}\right) \tag{8}$$

where ρ is the radial coordinate, and λ_0 is the design wavelength. The geometry leading to this

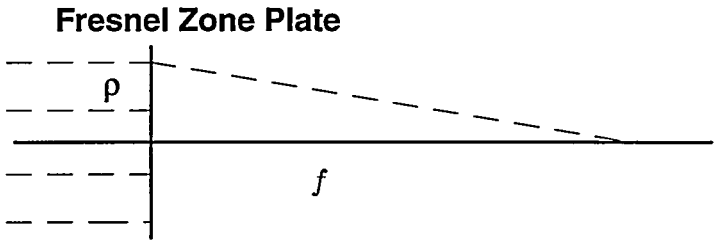

Figure 1. Conversion of a plane wave into a converging spherical wave by a kinoform formed on a plane surface.

expression is shown in Fig. 1.

This expression can be expanded into a Taylor series about $\rho = 0$ to yield:[8]

$$\Delta\phi(\rho)=\frac{2\pi}{\lambda_0}\cdot\left[-\frac{\rho^2}{2f_D}+\frac{\rho^4}{8f_D^3}-\frac{\rho^6}{16f_D^5}+\frac{5\rho^8}{128f_D^7}+\cdots\right]$$
$$=\frac{2\pi}{\lambda_0}\cdot\left[\alpha_1\rho^2+\alpha_2\rho^4+\alpha_2\rho^6+\alpha_4\rho^8+\cdots\right]. \tag{9}$$

One is not restricted to spherical phase functions, and the typical lens design program calculates the optimum α_i's to minimize the error function. However, to choose a good starting point, one or two coefficients should be calculated using the focal length for the diffraction portion of the hybrid found in the first order pre-design to provide some confidence that the automated design is proceeding correctly.

2.2 Location of Fresnel Zones for Planar Kinoforms

Once the designer and the program produce an optical design that sets the focal length of the diffractive optic, one needs to calculate the location of each zone, its optical depth, and optimum profile. We first examine the calculation of zone location for a diffractive optic placed on a plane surface. To constructively add to the image intensity with contributions from each Fresnel zone, the optical path difference between each zone must equal one (or integer multiples of one) wavelength. One must solve the following equation for the correct zone radii locations:

$$\frac{2\pi}{\lambda_0}\cdot\left(\sqrt{f_D^2+\rho^2}-f_D\right)=k\cdot 2\pi$$
$$\rho_k=\sqrt{2k\lambda_0 f_D+k^2\lambda_0^2}\approx\sqrt{2k\lambda_0 f_D}\approx\rho_1\sqrt{k} \tag{10}$$

where the approximations may be used when $\rho << f_D$. Note that the zone spacing varies as the square root of the index. The width of the first zone for our F/3.6 lens is 1.36 mm. To find the maximum number of zones needed for the diffractive surface, we let ρ_k equal the radius of the optic and solve for k_{max}. This becomes

$$k_{\max}=\frac{-f_D+\sqrt{f_D^2+\rho_{\max}^2}}{\lambda_0}\approx\frac{\rho_{\max}^2}{2\lambda_0 f_D} \tag{11}$$

where once again the approximation is quite close to the exact calculation when $\rho << f_D$. Our F/3.6 optic will require 84 zones for achieve the focal length of 1582.2 mm. One critical parameter that is necessary for tool selection and evaluating a potential design for suitability for diamond turning is the spacing of the outermost zone. It is found by calculating the integer k_{max} and then subtracting one to derive an expression for the index of the outermost zone minus one. This expression is then substituted into the expression for the zone radius found earlier. By subtracting this final expression from the maximum radius of the optic, we arrive at the minimum zone spacing required at the outermost diffractive zone:

$$\Delta\rho_{\min}=\rho_{\max}-\sqrt{\lambda_0^2-2\lambda_0\sqrt{f_D^2+\rho_{\max}^2}+\rho_{\max}^2}\,. \tag{12}$$

However, an estimate for the minimum zone spacing for slow optics can be expressed as:[9]

$$\Delta\rho_{\min}\approx\frac{\lambda_0(f_D+k_{\max}\lambda_0)}{\rho_{\max}}\approx 2\lambda_0 F/\#. \tag{13}$$

Therefore, the faster the diffractive lens needed for the hybrid optic, the smaller the minimum zone spacing for the diffracting grooves at the extreme edge of the optic. Since the phase shift between adjacent zones must be 2π to form an image point, it can be seen that the maximum phase depth for each groove must be

$$d_{zone} = \frac{\lambda_0}{n-1} \tag{14}$$

where it is assumed that the optic will be in air and constructed of material with index of refraction n. For the design in this paper, the diffractive portion has an F/# of F/63, so the minimum zone spacing at a design wavelength of 0.58756 μm is approximately 74.03 μm. By contrast, an F/10 diffractive optic at this wavelength would have a minimum outer zone spacing of 11.75 μm. In either case the maximum zone depth is 1.2 μm for acrylic.

2.3 Location of Fresnel Zones for Kinoforms on Arbitrary Surfaces

To exploit diamond turning (and optical design) to the fullest, one should not be restricted to placing kinoform optics on planar base surfaces. Since the optical path calculation is different for each kind of base surface, however, a general approach is needed to calculating the zone locations prior to the

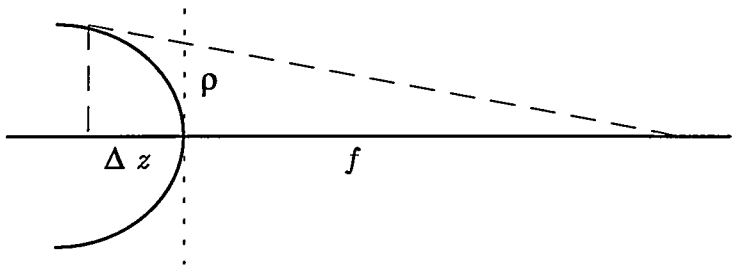

Figure 2. Diagram showing relationship between the focal length of the kinoform and the sag of an arbitrary base surface.

diamond machining operation. Figure 2 depicts the general case for computing zone location for kinoforms with arbitrary base surfaces. The phase difference as a function of radial coordinate with respect to the center of the optic may be written as

$$\Delta\phi(\rho) = \frac{2\pi}{\lambda_0} \cdot \left(f - \sqrt{(f+\Delta z)^2 + \rho^2} \right) \tag{15}$$

and where the sag (deformation of the surface along the optical axis in the Z-direction) of a general rotationally-symmetric aspheric surface may be expressed as

$$\Delta z = \frac{C\rho^2}{1+\sqrt{1-(1+\kappa)C^2\rho^2}} + a_1\rho^2 + a_2\rho^4 + a_3\rho^6 + a_4\rho^8 + \cdots. \tag{16}$$

Here, C is the curvature (reciprocal of radius of curvature) to the best-fit sphere, κ is the conic constant, and the a_i are the coefficients for the aspheric deformation terms. Note that this general asphere form is slightly different from that typically found in the literature[10] since a quadratic phase term is included with the aspheric deformation terms. If we now solve for the zone location as was done before for a planar base surface (for infinite conjugates) the result is:

(17) $$\rho_k = \sqrt{2 f_D k\lambda_0 + k^2\lambda_0^2 - 2 f_D \Delta z - \Delta z^2}\,.$$

When the sag is zero in the case of a plane surface, the zone location expression reduces to the form found earlier. Hazra *et al*[11] further simplified the expression above for the case of a spherical base surface obtaining

(18) $$\rho_k = \sqrt{2k\lambda_0 f_D + k^2\lambda_0^2 - 2k\lambda_0 R\left(1 + \frac{k\lambda}{R} - \sqrt{1 - 2(f_D - R)\frac{k\lambda_0}{R^2}}\right)}$$

and it can be shown that in the limit as R approaches infinity (a plane surface), the above expression becomes that previously found for a planar base surface.

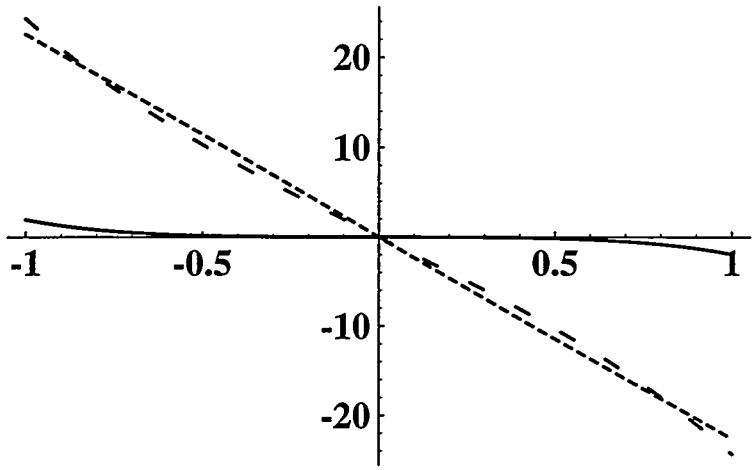

Figure 3. Ray fan plot of the tangential section showing ray heights in microns versus normalized exit pupil coordinates. Middle wavelength (d) shown as a solid line, the short wavelength (F) as the small dashed line, and the long wavelength (C) as the long dashed line.

3. Translation of Optimized Design for Diamond Turning

With the design parameters determined by the first order pre-design, a hybrid singlet can be designed with the aid of most commercial lens design programs using a binary optic or computer generated hologram surface. The basic lens design caveats using automatic design programs should be observed[12]. In practical designs that incorporate hybrid elements, the diffractive surface is intended only to achromatize the optic, and indiscriminate use of the phase function as a variable during the optimization process may lead to spherochromatism. Following Wood's approach[13], we design the singlet with an aspheric front surface for correction of spherical aberration, and determine the optimum shape of the rear surface for coma correction, leaving the diffractive surface to correct primary longitudinal chromatic aberration. We first describe the results of the automated design and summarize its performance. The approach to translating the optical parameters found from the lens design program into a form amenable to diamond turning is then described.

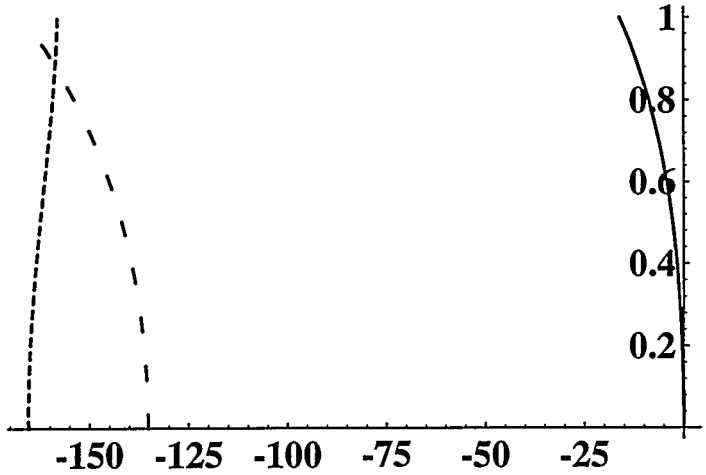

Figure 4. Longitudinal aberration plot of the hybrid singlet showing secondary spectrum. The solid line depicts center wavelength (d) performance, the short dashed line shows the short wavelength (F) image plane location, while the long dashed line showing the normalized exit pupil coordinates versus optical axis location of the image plane in units of μm for long wavelength light (C).

3.1 Hybrid Singlet Design

The hybrid lens was designed using a commercial lens design program. It has an F/# of 3.6 with an element diameter of 25 mm, and was optimized only for on-axis performance. The final shape was that of a positive meniscus lens having 5 mm thickness, with the aspheric first surface facing the object having radius of curvature +43.14 mm, and a conic constant of -0.5338. No significant improvement could be found by allowing higher-order aspheric terms to vary. An angle solve was used at the second surface to maintain the design F/#, which resulted in a spherical second surface with radius of curvature +463.54 mm. A marginal ray height solve was used to find the paraxial image plane, 87.12 mm from the second surface of the lens. A single coefficient was retained for the binary phase surface used in the design of the diffractive surface of the hybrid lens, and was found to be -3.4524×10^{-4} mm^{-1}. Although the marginal ray height solve does not result in the "best focus," it illustrates the secondary spectrum more vividly in the ray fan plot (Fig. 3), seen to amount to approximately 20 μm of transverse error. Secondary spectrum can be approximated to first order using the relationship[14]:

$$\frac{\partial f'}{f'} = -\frac{\Delta P}{\Delta \nu} \tag{19}$$

where P is the partial dispersion of the element, and ν is its relative reciprocal dispersion (Abbe Number). For acrylic, the partial dispersion and Abbe number are 0.3070 and 57.2, respectively, while the diffractive surface has partial dispersion and Abbe number of 0.4038 and -3.45. The focal length-normalized longitudinal shift in focus is calculated to be about 1.596×10^{-3}, which is confirmed in the longitudinal aberration plot shown in Fig. 4.

3.2 Interpreting Optical Design Parameters for Diamond Turning

3.2.1 Calculation of the Equivalent Phase Surface for the Kinoform

Based on the speed of our designed lens, only the quadratic coefficient from the binary phase function is required to adequately achromatize the hybrid singlet. The first coefficient is then used to calculate the focal length of the diffractive surface as found by the lens design program. To begin for the general case, we simply equate the phase function coefficient found from the lens design program with the first term found in the expansion of the spherical wave:

$$\alpha_1 = -\frac{1}{2f_D} \qquad (19)$$
$$f_D = -2\alpha_1 .$$

This diffractive focal length can now be used to compute the zone locations for the kinoform optic on an arbitrary base surface using the expressions found earlier.

Once the kinoform zone locations are determined, the form of the refractive "parent" surface necessary to produce the equivalent phase shift as the diffractive phase function must be calculated. Another way of viewing the refractive properties of a lens is to appeal to the wave nature of light and to consider the lens as a phase structure using an approach similar to Goodman[15]. A plane wave incident upon a refractive lens will undergo a differential phase shift as a function of radial coordinate, which depends on the sag of the optical surface. For a spherical surface, the sag can be expressed as:

$$\Delta z = R - \sqrt{R^2 - \rho^2} \qquad (20)$$

where R is the radius of curvature of the surface and ρ is the radial coordinate. The phase shift for an air-incident lens having index of refraction n can be written:

$$\phi(\rho) = \frac{2\pi}{\lambda_0}\cdot\left[n(\Delta_0 - \Delta z) + \Delta z\right] \qquad (21)$$
$$= -\frac{2\pi}{\lambda_0}\cdot(n-1)\cdot\Delta z + \frac{2\pi}{\lambda_0}\cdot\Delta_0$$

where Δ_0 is the optical path length of the lens at its center. This term is neglected since it is constant. As was done for the phase function produced by the diffractive surface, the sag for a spherical surface may be expanded into a Taylor series and combined with the result found above to compute the phase transformation brought about by the refractive surface:

$$\Delta\phi(\rho) = -\frac{2\pi}{\lambda_0}(n-1)\left[\frac{\rho^2}{2R_D} + \frac{\rho^4}{8R_D^3} + \frac{\rho^6}{16R_D^5} + \frac{\rho^8}{128R_D^7} + \cdots\right]. \qquad (22)$$

If the quadratic terms in the refractive and diffractive phase functions are equated, the necessary radius for the parent refractive optic can be found to achieve the correct diffractive focal length:

$$(n-1)\frac{\rho^2}{2R_D} = \frac{\rho^2}{2f_D} = -\alpha_1\rho^2 \qquad (23)$$
$$R_D = (n-1)\cdot f_D = -\frac{(n-1)}{2\alpha_1}.$$

For the first order predesign for the F/3.6 hybrid singlet, the radius of the parent refractive surface is found to be 776.9 mm, while the radius due to the automated design is 711.1 mm. However, Eq. (23) is

valid only for a kinoform placed on a plane surface. In general, one must find the equivalent refractive surface that maps the kinoform on a curved base surface into the phase function found from the lens design program. That is, one needs to solve the following equation:

$$-(n-1)\cdot\Delta z_{base}+\Phi=\alpha_1\rho^2 \tag{24}$$

where Φ is the phase function that must be provided by the equivalent refractive or parent surface. It was shown that the parent surface for the kinoform portion of the hybrid optic is simply $(n - 1)\,\Delta z_{kinoform}$. The equation to be solved for the parent diffractive surface on a base surface with arbitrary curvature is:

$$\begin{aligned}\alpha_1\rho^2 &= -(n-1)\left(\Delta z_{base}-\Delta z_{kinoform}\right)\\ \Delta z_{kinoform} &= \frac{\alpha_1\rho^2}{n-1}+\Delta z_{base}\end{aligned} \tag{25}$$

where the propagation constant k has been eliminated from both sides of the equation. If the paraxial expression for the sag is substituted for the base and kinoform terms, the equation becomes:

$$\alpha_1\rho^2=-(n-1)\cdot\frac{\rho^2}{2}\left(\frac{1}{R_{base}}-\frac{1}{R_{kinoform}}\right). \tag{26}$$

This equation can be solved for the radius of the parent surface of the kinoform, yielding:

$$R_{kinoform}=\frac{R_{base}}{\frac{2\alpha_1 R_{base}}{n-1}-1}. \tag{27}$$

Note that in the limit, as the base radius approaches infinity, the radius of the kinoform parent surface reduces to that found earlier in Eq. (23). Londoño and Clark[16] present a practical method for finding the radius of this surface using commercial lens design software by freezing all other variables in the design and changing the surface type to a Fresnel lens having an arbitrary base surface. The radius of the Fresnel lens found by the lens design software will be essentially the same as that found by Eq. (26). If one does not access to optical design software that permits the design of Fresnel lenses on arbitrary base curves, simply adding another thin element made of the same optical material and letting the optimization function find the best radius of curvature and conic constant will have the same effect. For the general case, suppose that the second surface is a conic section having the form:

$$\Delta z=\frac{C\rho^2}{1+\sqrt{1-(1+\kappa)C^2\rho^2}} \tag{29}$$

where C is the curvature and, ρ is the radial coordinate, and κ is the conic constant. Equating the phase function of the general conic for the equivalent phase surface with the phase function for the base surface plus the kinoform phase function, one can expand both sides into a Taylor Series and equate terms to find the curvature needed for the equivalent refractive surface for the actual kinoform as well as its conic constant. The equations that result are:

$$C_{diffractive} = \frac{2\alpha_1}{n-1} + C_{base}$$

(30)

$$\kappa_{diffractive} = \left(\frac{C_{base}}{C_{diffractive}} \right)^3 (1+\kappa_{base}) - 1.$$

Note that in the limiting case of a planar base surface, the curvature necessary for the diffractive portion reduces to that found earlier, and its conic constant is equal to -1, a parabola, as it must.

3.2.2 Zone Locations for the Designed Kinoform

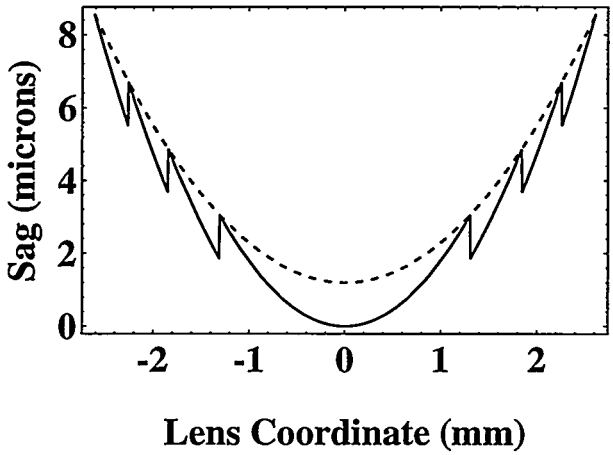

Figure 5. Shape and base curvature for the first four zones of the designed kinoform on the second surface of the hybrid optic. The base curve is depicted with dashed line and the image is in the positive direction (up) in this graph.

Using the expression defined in Eq. (15), one can calculate the zone locations of the kinoform surface for the infinite conjugate solution. Since a spherical surface was sufficient for the second surface of the hybrid, the radius for the parent surface of the diffractive optic is found to be 1331.53 mm. The conic constant term can be ignored since the denominator approaches one as this is an F/53 surface, and the paraxial expression of Eq. (27) is adequate. This will usually be the case when the kinoform diffractive surface is used solely for achromatization. To calculate the shape of kinoform, one can use the expression published by Londoño in Ref. 2 and superimpose on it the profile of the base curve, with the results shown in Fig. 5 for the first four zones. Figure 6 shows the details of the last four zones, showing the 68.2 μm spacing at the outermost zone. The maximum number of zones is found by using the expression in Eq. (18) and setting it equal to the full radius, 12.5 mm. The maximum number of zones is almost 92 (91.8), which is somewhat greater than the 84 calculated for the first order design. The mechanics of how this design may be diamond turned is treated in the next section.

3.3. Diamond Turning Issues

Examining Figs. 5 and 6, the approach to cutting the optic is straightforward. The second surface is machined to establish the base curvature for the kinoform. The tool path generator is then set for the radius of curvature for the parent optic of the kinoform, 1331.53 mm. These coordinates are added to those of the base curve, and at each zone index, the tool is withdrawn one phase depth (1.2 μm)

that is calculated using Eq. (14), and the process repeated at each zone transition until the center of the optic is reached. The cutting tool has a finite radius, which makes the machined optic deviate from its ideal form. In the next section, the issues of tool selection as they impact surface finish, cutting time and

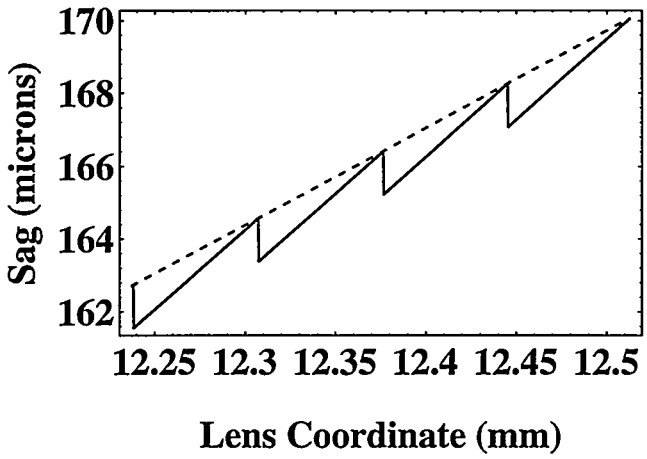

Figure 6. Last four zones of the hybrid optic with base curve superimposed using the dashed line. Note the spacing at the outermost zone is 68.2 μm.

diffraction efficiency are examined so that the fabrication of the optic may be realized.

3.3.1. Optimum Tool Selection

Proper tool selection is driven by the minimum feature to be machined, the required surface finish, diffraction efficiency, feed rate, spindle speed, and the allowable time for machining based on throughput requirements and dimensional stability of the cutting platform.

To machine the aspheric first surface and spherical rear surface, a controlled-radius single-point diamond cutting tool will be used. The theoretical finish equation is[17]:

$$PV_{\text{surface finish}} = \frac{f^2}{8R_{tool}} \tag{31}$$

where f is the feed per revolution and R_{tool} is the tool radius. The focus here will be on the cutting of the kinoform surface since this is the most challenging part of the project and drives the maximum tool radius based on the outermost zone width and phase depth. Figure 7 shows the progression of a 25 μm full radius tool as it cuts the kinoform shape on the base curve of the second surface. For this design, it appears that the 25 μm tool will work well. One can help the situation by using a 25 μm half-radius tool that will vastly improve the fidelity with which the phase step can be cut at the zone transition. Should further improvement be necessary, the transition areas can be touched up with a 2 μm-wide flat-surfaced tool.

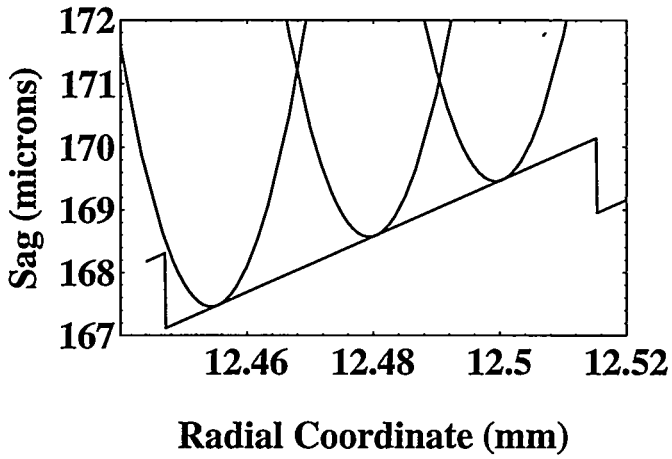

Figure 7. Machining of kinoform on the base curve showing the tool clearance at the phase step for the outermost zone of the hybrid optic and the progression of three tool positions. The tool shown has a 25 μm radius and is drawn to the same scale as the kinoform.

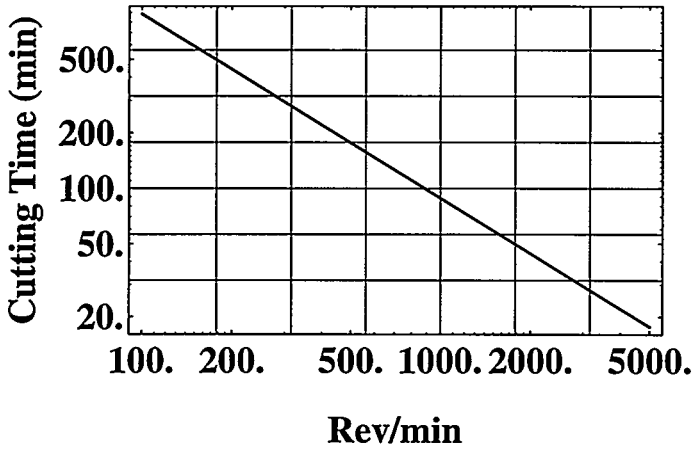

Figure 8. Log-log plot of cutting time in minutes versus the spindle speed in revolutions per minute.

3.3.2. Feed Rate, Spindle Speed and Cutting Time

Since instrumental errors will swamp the theoretical surface finish, a goal of 1 Å peak-to-valley is used to calculate the feed rate required, now that the tool radius has been selected, resulting in a feed of 0.14 μm per revolution of the spindle. The radius of the optic is 12.5 mm, and Fig. 8 plots cutting time versus spindle speed so that a proper choice can be made, based on throughput requirements and material limitations, i.e. glass temperature, cutting fluids permitted, and the thermal stability of the diamond turning platform. For the feed rate calculated above, 90 minutes is required to cut the kinoform surface at 1000 spindle revolutions per minute.

3.3.3. Impact of Tool Radius on Diffraction Efficiency

Reidl[18] has addressed the issues involved in diamond-turning hybrid optics for the infrared, and uses a figure of merit called *energy blockage*. Examination of Fig. 7 shows that a fillet will occur at the zone transition due to the finite radius of the diamond tool. Since the phase step that is cut is not abrupt and hence imperfect, light is not diffracted efficiently into the correct order at the design wavelength. This effect is separate from the theoretical efficiency possible from a diffractive surface as a function of wavelength, groove spacing and blaze profile that is treated in Ref. 16. Riedl calculates the area in the annulus formed at each zone transition, sums the areas for all zones, and finds the ratio of the area due to the summed annuli to the total area of the lens, using this as the blocked energy figure of merit. Using a half-radiused tool should nearly eliminate this reduction in diffraction efficiency, especially if the zones are cleaned up with a so-called dead sharp tool. However, even if the full-radiused tool were used having a radius of 25 μm, an energy blockage of only 7.3 % would result.

4. Conclusion

The progress of an effort at Oak Ridge National Laboratory has been presented summarizing efforts at fabricating a hybrid refractive/diffractive singlet using single-point diamond turning that is designed to function in the visible portion of the spectrum. The aim is to push the state-of-the art in deterministic fabrication of hybrid optical elements by exploiting all of the degrees of freedom available in the design and possible using diamond turning: aspheric surfaces, along with the kinoform surface (as opposed to a binary approximation) formed on a base surface having arbitrary shape. The attempt here is to summarize the considerable quantity of information available in the literature on the design (and to a lesser extent fabrication) of hybrid lenses while concentrating on practical approaches of design and fabrication of these devices.

Although the limitations of diamond-turning are well documented, the ability to fabricate hybrid optical elements using deterministic methods that have adequate quality for a broad spectrum of consumer and military applications in the visible and near infrared will have far-reaching consequences. Mass replication using diamond-turned molds will be more attractive due to the ability to achromatize optical elements or systems made of a single optical material. Although one usually thinks in terms of optical plastics for mass replication, including the limitations inherent in these materials, recent advances in the bulk casting of sol-gel glass give the optical designer and manufacturer a high-quality optical material (silica glass) to mate with the emerging technology of hybrid optics.

5. Acknowledgment

This research was done in support of work performed by Martin Marietta Energy Systems, Inc. for the U.S. Department of Energy under contract DE-AC05-84OR21400.

6. References

[1]Clark, P. P. and C. Londoño, "Production of kinoforms by single point diamond machining," *Optics and Photonics News*, **15** (12), 39-40 (1989).

[2]Londoño, C., W. T. Plummer, and P. P. Clark, "Athermalization of a single-component lens with diffractive optics," *Appl. Opt.*, **32** (13) 2295-2302 (1993).

[3]ZEMAX-EE, Focus Software, Inc., P. O. Box 18228, Tucson, AZ 85731-8228.

[4]Smith, W. J., Modern Optical Engineering: The Design of Optical Systems, 2nd Ed., (McGraw Hill, Inc, New York, 1990), p. 78.

[5]Welford, W. T., Aberrations of Optical Systems, (Adam Hilger, Bristol, 1986), p. 194.

[6]Stone, T. and George, N., "Hybrid diffractive-refractive lenses and achromats," *Appl. Opt.*, **27** (14) 2960-2971 (1988).

[7]Born, M. and Wolf, E. Principles of Optics, 6th Ed., (Pergamon Press, Oxford, 1986), pp. 175-178.

[8]Abramowitz, M. and Stegun, I. A., Handbook of Mathematical Functions, (NBS Appl. Math. Series 55, 1964), p. 14.

[9]Nishihara, H. and T. Suhara, "Micro Fresnel Lenses," Chap. 1 in Progress in Optics XXIV, E. Wolf, Ed., (Elsevier, Amsterdam, 1987), 3-37 .

[10]Malacara, D., "An Optical Surface and Its Characteristics," Appendix 1 in Optical Shop Testing, 2nd Ed., D. Malacara, Ed. (John Wiley, New York, 1992).

[11]Hazra, L. N., Y. Han, and C. Deslile, "Curved kinoform lenses for stigmatic imaging of an axial object at infinity," *Opt. Comm.*, **90**, 201-206 (1992).

[12]Smith, W. J. "Automatic Lens Design: Managing the Lens Design Program," Chap. 2 in Modern Lens Design- A Resource Manual, (McGraw Hill, New York, 1992).

[13]Wood, A. P. "Design of infrared hybrid refractive-diffractive lenses," *Appl. Opt.* **31** (13), 2253-2258 (1992).

[14]Stone, T. and N. George, "Hybrid diffractive-refractive lenses and achromats," *Appl. Opt.*, **27** (4), 2960-2971 (1988).

[15]Goodman, J. W., Introduction to Fourier Optics, (McGraw-Hill, New York, 1968), pp. 77-83.

[16]Londoño, C. and P. P. Clark, "Modeling diffraction efficiency effects when designing hybrid diffractive lens systems," *Appl. Opt.,* **31** (13), 2248-2252 (1992).

[17]Sanger, G. M., "The Precision Machining of Optics," in Applied Optics and Optical Engineering, R. R. Shannon and J. C. Wyant, Eds., Vol. X, (Academic Press, San Diego, 1987).

[18]Riedl, M. J., "Predesign of diamond-turned refractive/diffractive elements for IR objective," in Lens Design, *SPIE Critical Reviews in Optical Engineering*, **CR41**, 140-157 (1992).